ACS APPLIED MATERIALS & INTERFACES

www.acsami.org Research Article

Soft and Stretchable Thermoelectric Generators Enabled by Liquid Metal Elastomer Composites

Mason Zadan,[⊥] Mohammad H. Malakooti,[⊥] and Carmel Majidi*

Cite This: *ACS Appl. Mater. Interfaces* 2020, 12, 17921−17928 Read Online

ACCESS | Metrics & More | Article Recommendations | Supporting Information

ABSTRACT: Stretchable thermoelectric generators (TEGs) capable of harvesting electrical energy from body heat under cold weather conditions have the potential to make wearable electronic and robotic systems more lightweight and portable by reducing their dependency on on-board batteries. However, progress depends on the integration of soft conductive materials for robust electrical wiring and thermal management. The use of thermally conductive soft elastomers is especially important for conforming to the body, absorbing body heat, and maintaining a temperature gradient between the two sides of the TEGs in order to generate power. Here, we introduce a soft-matter TEG architecture composed of electrically and thermally conductive liquid metal embedded elastomer (LMEE) composites with integrated arrays of n-type and p-type Bi_2Te_3 semiconductors. The incorporation of a LMEE as a multifunctional encapsulating material allows for the seamless integration of 100 thermoelectric semiconductor elements into a simplified material layup that has a dimension of 41.0 × 47.3 × 3.0 mm. These stretchable thermoelectric devices generate voltages of 59.96 mV at Δ10 °C, 130 mV at Δ30 °C, and 278.6 mV and a power of 86.6 $\mu W/cm^2$ at Δ60 °C. Moreover, they do not electrically or mechanically fail when stretched to strains above 50%, making them well-suited for energy harvesting in soft electronics and wearable computing applications.

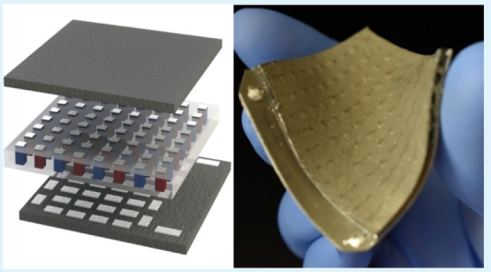

KEYWORDS: *thermoelectric wearables, liquid metal, stretchable electronics, thermoelectric energy harvesting, liquid metal embedded elastomer, multifunctional composites, thermal interface, stretchable thermoelectric generator*

INTRODUCTION

Thermoelectric generators (TEGs) are a simple and effective way to harvest excess (and otherwise wasted) energy from body heat in order to power wearable sensors and circuitry.[1−4] These devices have been shown to have the potential to power a myriad of electronic devices including implantable medical devices, internet of things (IoT) technologies, wireless body area networks, and wearable devices for applications ranging from glucose sensing to global positioning system tracking.[5−11] While promising for some use cases, existing wearable TEG technologies are primarily made of rigid or inextensible materials that limit their ability to conform to the skin or support repeated mechanical deformation.[12] For wearable applications, reliable heat absorption is greatly improved through the use of flexible materials to fabricate TEGs that can conform to the skin and accommodate natural human motion. Previous studies have incorporated polydimethylsiloxane (PDMS) and polymers in order to replace more rigid materials, resulting in flexible TEGs that are more compatible with the body.[13−15] One such study used PDMS as a matrix material along with rigid semiconductors that were connected using copper interconnects.[16] This resulted in a flexible and bendable TEG, although performance was limited to an electrical power output of 2.1μW when exposed to a temperature difference of ΔT = 19 °C. A more recent study on thermoelectric devices (TEDs) for limb cooling aligned semiconductors between two elastomer sheets in the open air, thereby mitigating the thermal conductivity between the top and bottom elastomer pieces.[17] A separate study introduced a flexible PDMS TEG composed of an array of 144 bismuth telluride semiconductor chips wired together using thin, flexible, and yet inextensible copper interconnects. This TEG was combined with a boost converter in order to power a device capable of electrocardiography, thereby showing the potential of flexible TEGs for wearable biomonitoring and electronics applications.[18,19]

The drawbacks in these and other previous elastomer-based soft TEGs follow from the use of PDMS as an encapsulating material. PDMS is a thermal insulator with a low thermal conductivity of 0.18 W m^{-1} K^{-1} that has the potential to interfere with the flow of heat to and from the thermoelectric modules.[20] Moreover, wiring the thermoelectric components with rigid or inextensible electrical interconnects results in a

Received: November 2, 2019
Accepted: March 25, 2020
Published: March 25, 2020

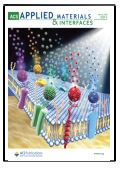

Downloaded via CARNEGIE MELLON UNIV on December 22, 2023 at 20:32:08 (UTC).
See https://pubs.acs.org/sharingguidelines for options on how to legitimately share published articles.

© 2020 American Chemical Society

https://dx.doi.org/10.1021/acsami.9b19837
ACS Appl. Mater. Interfaces 2020, 12, 17921−17928

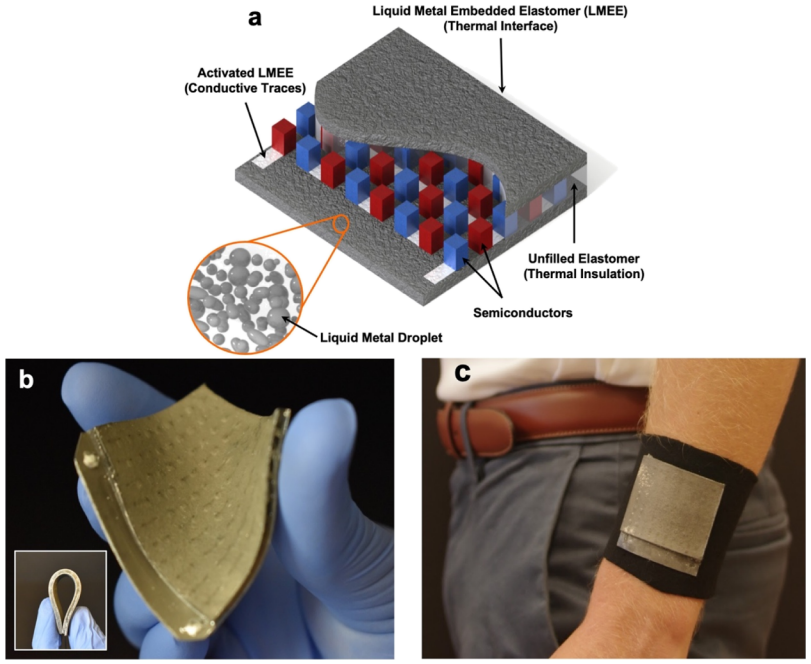

Figure 1. Stretchable TEGs with a LM embedded elastomer (LMEE). (a) A schematic of the stretchable TEG with a thermally conductive LMEE as the material interface on the top and bottom. The LMEE contains a mechanically sintered pattern for providing electrical connections between p-type and n-type Bi_2Te_3 semiconductors. (b) A photo of the fabricated TEG under deformation (inset: a TEG device completely bent). The raised bumps on the surface of the TEG are the locations of the LMEE conforming around the semiconductors. (c) Stretchable TEG conforming to the forearm when attached to a fabric armband.

device that cannot stretch and fully conform to the body. Since rigid interconnects cannot deform with the surrounding elastomer, they can induce high stress concentrations that can lead to fracture or delamination and consequently mechanical or electrical failure of the device. Progress toward the development of mechanically robust TEGs for wearable computing depends on the use of soft and stretchable materials for thermally conductive encapsulation and internal electrical wiring.

Gallium-based liquid metal (LM) alloys such as eutectic gallium−indium (EGaIn) and gallium−indium−tin (Galinstan) are a promising class of materials for addressing existing challenges in creating soft and stretchable TEGs. The high electrical conductivity and ability of EGaIn to deform and move with the surrounding materials makes it an excellent candidate as a conductive material for stretchable electronic devices.[21−25] This unique ability of EGaIn has been incorporated in simple applications for TEGs to aid as the interconnects between semiconductors.[26,27] In one such study, EGaIn channels were embedded within PDMS and functioned as electrical interconnects connecting the TEG semiconductors.[28] Besides the complex fabrication process, the resulting TEG exhibited limited voltage and power generation (8.22 mV and 46.28 μW, respectively, for a Δ30 °C temperature difference) but demonstrated that EGaIn is a promising material for electrical interconnects in such applications. Similar to previously reported flexible TEGs, the major drawback was the poor thermal management in the device because of the low thermal conductivity of the encapsulating elastomer. More recently, the design of TEGs with EGaIn channels was improved by enhancing the thermal conductivity of pure PDMS.[29]

Alternatively, LM alloys have been incorporated into flexible and stretchable devices by suspending LM micro/nanodroplets within an elastomeric matrix. Such LM-embedded elastomers (LMEEs) have been shown to exhibit exceptional electrical and thermal properties with a wide range of applications.[30] LMEEs have also been shown to operate effectively under extreme cold weather conditions because of the supercooling effects that suppress the freezing temperature of LM alloys encased in this elastomer composite from −5.9 to −84.1 °C. This freezing point suppression addresses operating challenges in LM alloy based TEGs in cold weather environments.[31] Particularly for TEG applications, it was recently shown that utilizing LMEE thermal interfaces rather than insulating elastomers significantly improves the energy harvesting performance of TEGs.[31] Here, we show that stretchable high performance TEGs can be simply designed and fabricated by utilizing LMEE composites both as a stretchable circuit wiring and a thermally-conductive elastomer for more efficient heat management.

In this paper, we introduce a soft and stretchable TEG for cold weather conditions that utilizes an electrically insulating and conductive LMEE for thermal management and electrical connectivity between embedded, milli-scale Bi_2Te_3 components. As shown in Figure 1a, the device is composed of a top and bottom LMEE layer that acts as a heat spreader and forms electrical interconnects between the Bi_2Te_3 chips when mechanically sintered. The LMEE layers are composed of LM droplets dispersed in a soft silicone elastomer matrix. Their high elastic compliance and thermal conductivity enable the layers to conform intimately to the skin and transport heat through the embedded thermoelectric components. Moreover, the LMEE can be locally "sintered" with mechanical activation in order to create electrically conductive traces on the normally electrically insulating LMEE that makes connections between the embedded semiconductor components, thereby eliminating the need for additional components to individually connect

https://dx.doi.org/10.1021/acsami.9b19837
ACS Appl. Mater. Interfaces 2020, 12, 17921−17928

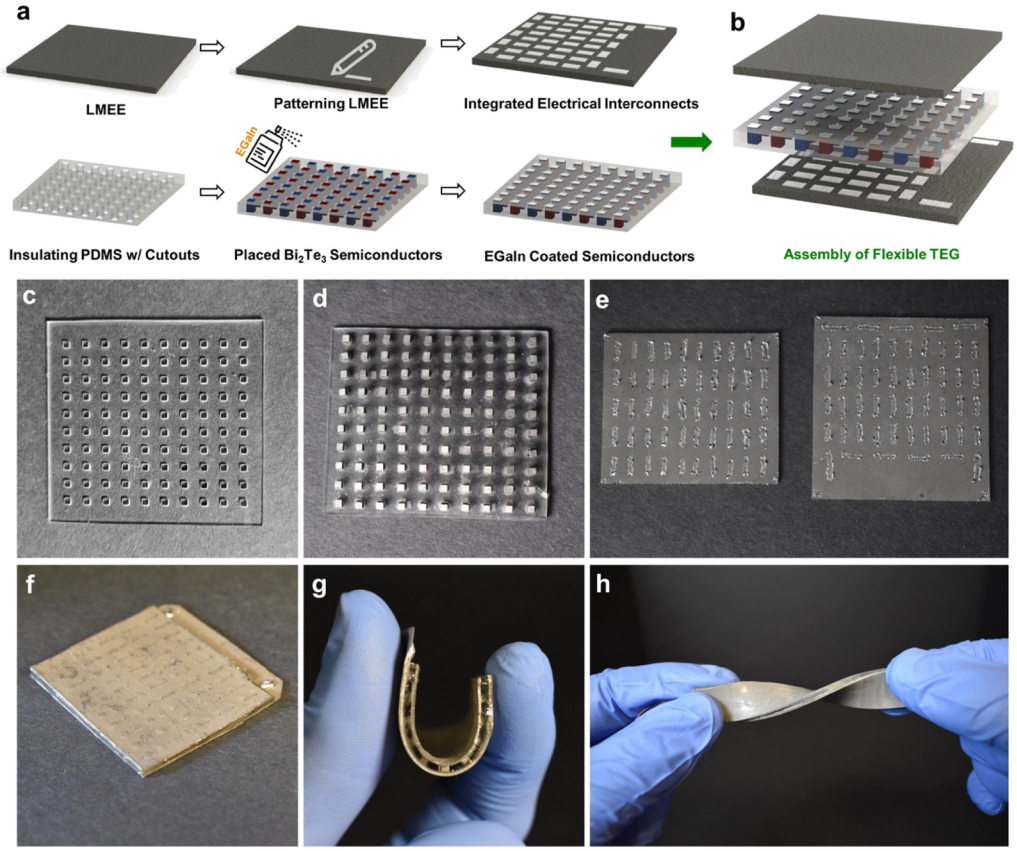

Figure 2. Fabrication process of the stretchable TEG with LM composites. (a) Fabrication schematic highlighting the creation of the semiconductor interconnects through LMEE mechanical activation along with EGaIn sputtering onto the semiconductor array. (b) Schematic of TEG assembly once the internal side of LMEE layers is oxygen plasma treated. (c) The laser cut PDMS center layer with cutouts for the semiconductors. (d) Insulating center layer of PDMS with one hundred Bi_2Te_3 semiconductors in P and N alternating alignment. (e) Patterned top (left) and bottom (right) LMEE pieces, the patterns will serve as electrical connections between individual semiconductors. (f) Assembled 42 × 48 mm stretchable TEG with raised bumps indicating alignment and position of semiconductors. (g) Side view of the TEG bending 180° with semiconductors visible and deforming with the device (h) Photograph of a TEG post 1000 loading cycles with no damage or hysteresis.

the semiconductors. Specifically, the electrically conductive LMEE traces eliminate the need for rigid copper interconnects that would otherwise be required for serial connection of the semiconductors. Because the LMEE serves two crucial functions in the TEG device and reduces the number of required components in the device, the fabrication process is significantly simplified. Moreover, because the device is primarily composed of soft and stretchable elastomers, these TEGs are highly flexible (Figure 1b) and can be strained to over 50% in tension without electrical or mechanical failure, exceeding the strain limit of previous TEGs and well above the deformation needed for wearable electronic applications. Furthermore, they exhibit only a small increase in resistance when stretched and do not permanently deform because of repeated cyclic loading. Such advantages give the TEGs presented here the ability to remain functional while bending and stretching in order to conform to the body (Figure 1c).

RESULTS AND DISCUSSION

Figure 2a,b illustrate the steps of the fabrication process. The overall structure of this device consists of three main components: a top and bottom layer of the LMEE and an insulating PDMS center layer embedded with an array of semiconductors. LMEE's excellent thermal conductivity and electrical properties lend itself well for this device since the material can act as a conformable area of contact for heat absorption and also as an array of electrical interconnects between the semiconductors. In particular, LMEE composites with a 50% LM volume fraction have a thermal conductivity of 1.6 $W{\cdot}m^{-1}{\cdot}K^{-1}$ in their unstretched state, which makes them excellent for thermal absorption.[32] A 50% fill percentage was selected for these devices because the thermal conductivity of the LMEE is a function of the fill percentages of the LM alloy, with an increase in the fill percentage corresponding to an increase in thermal conductivity.[32] Specifically, 50% has been shown to work well for not only thermal but also electrical applications.[33] This fill percentage is high enough to create percolating networks when sintered with an excellent conductivity of $\sigma = 1.37 \times 10^5$ S m^{-1} but low enough to be electrically insulating when not activated as shown in a previous work.[33,34] These bismuth telluride semiconductors were selected for their high efficiency and figure of merit (ZT) of ≥1.1 at 300 K. High efficiency is a relative term—for example, high performance Bi_2Te_3 semiconductors with a ZT = 1 at Δ 50 °C have an efficiency of only around 3.5%. This indicates the importance of selecting appropriate thermal materials when developing a TEG device.[35] Comparing these semiconductor's figure of merit with those reported in the literature for Bi_2Te_3 semiconductors, the figure of merit of these devices at 300 K is in line and comparable to those of other semiconductors making them an excellent choice for thermoelectric energy harvesting.[36−38] Referring to Figure

https://dx.doi.org/10.1021/acsami.9b19837
ACS Appl. Mater. Interfaces 2020, 12, 17921−17928

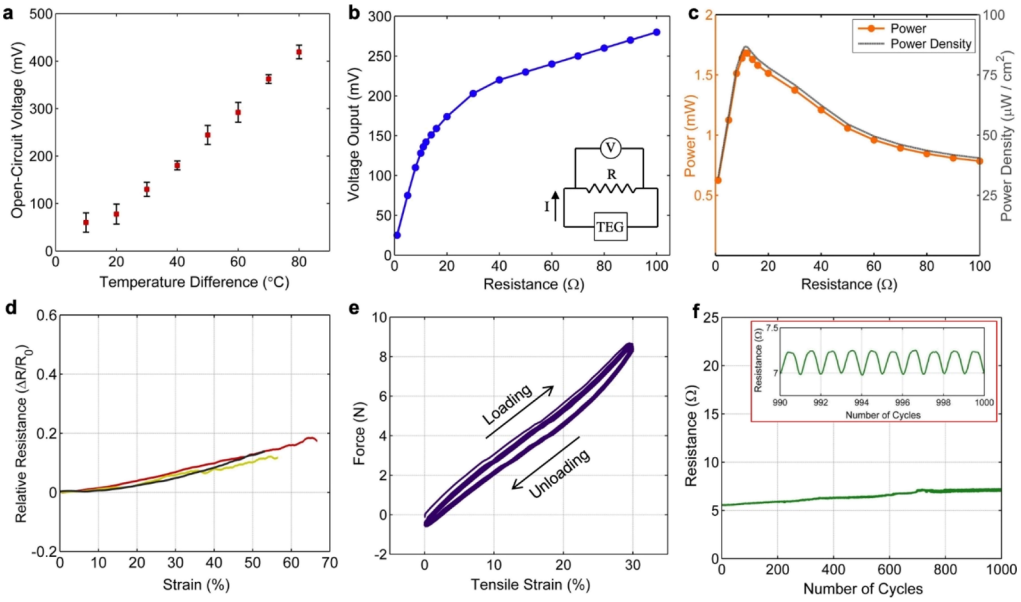

Figure 3. Energy harvesting and electromechanical characterization of stretchable TEGs. (a) The open circuit voltage as a function of the temperature gradient on the top and bottom of the TEGs. (b) The output voltage as a function of external resistor load for a temperature gradient of 60 °C. (c) Estimated power and power density across the varying external resistor load for the 60 °C temperature difference. (d) Change in relative resistance as a function of tensile strain for three representative stretchable TEG devices. (e) Hysteresis behavior of the soft-matter TEG under cyclic loading up to 1000 cycles. (f) Measured electrical resistance of the stretchable TEG subjected to uniaxial cyclic loading with maximum strain of 30% for 1000 cycles; (inset: zoomed-in view for the last 10 cycles).

2c,d, P and N-type semiconductors were placed in the alternating order in one hundred square holes that were patterned within a layer of PDMS (Sylgard 184, Dow Chemicals). To decrease contact resistance caused by the semiconductors and interconnects, EGaIn was sputtered on the top and bottom of the semiconductors. To selectively deposit the EGaIn, a flexible stencil was placed on both sides of the center PDMS structure with cutouts for the semiconductors. EGaIn was airbrushed on the top and bottom and the stencil was removed leaving EGaIn only on the ends of the semiconductors. Details of the fabrication of the LMEE and thermoelectric layers are presented in the Experimental Methods section.

To achieve electrical connection between the embedded semiconductors, internal interconnects were created by mechanically activating the LMEE composite. By applying constant force, the suspended EGaIn droplets are ruptured internally to create conductive pathways for electrical circuitry.[34] When activated, these pathways can have a volumetric conductivity as high as $\sigma = 1.37 \times 10^5$ S m^{-1}, therefore being conductive enough to replace copper or other rigid conductors and thereby greatly cutting down on the complexity of fabrication.[33] In this application, pressure from a pen was used to activate the LMEE and create electrical interconnects between the adjacent semiconductor legs. This mechanical patterning was performed on the top and bottom LMEE layers in order to support the array of 100 semiconductors (Figure 2a,e).

After interconnect patterning, the elastomer pieces were bonded together with the aid of oxygen plasma treatment (SPI Plasma Prep II) in order to activate the surfaces and allow for strong adhesion.[39,40] Following the plasma treatment, the three pieces were manually aligned and bonded together. Glass slides were placed on the top and bottom of the device and a clamp held the device together. It was finally cured in an oven for 1 h at 100 °C. Figure 2f gives a view of the cured TEG with a final dimension of 41.0 × 47.3 × 3.0 mm in which the raised dots and darkened lines on the surface highlight the semiconductor placement and sintered interconnect pathways, respectively. The embedded semiconductors and interconnects, deforming along with this TEG, can move and operate reliably under extreme strain such as the positions in Figure 2g,h in which the semiconductors are highlighted along the side view (Figure 2g). Figure 2h highlights the lack of damage, hysteresis, or tearing after 1000 cycles of 30% for these TEGs.

In order to understand the thermoelectric performance of these stretchable TEGs, the open-circuit voltage was measured as a function of the temperature difference between the two sides of the stretchable TEG devices. Figure 3a shows the increase of the open circuit voltage as the temperature gradient increases. Voltage was measured by placing the TEG on a hot plate at varying discrete temperatures from 35 to 105 °C with increments of 10 °C. Longer exposure of the TEG on the hotplate amounted to a loss in voltage. This occurred much more quickly at higher temperatures, as the heat transferred from the bottom of the TEG to the top more quickly lowering the temperature gradient. Additional details of the method for measuring the voltage output are presented in the Experimental Methods section.

Figure 3a shows the data for four cycles of heating starting at ΔT = 10 °C and increasing to a temperature difference of 80 °C. The top side of the TEG was kept at room temperature (approximately 25 °C) for each test and the TEG surface temperature was tested using an infrared camera (FLIR C2, FLIR Systems Inc.) in between tests. The results indicated high voltage outputs that are well within the range needed for wearable electronics, even at lower temperature gradients. For example, the average voltage output for a 10 °C temperature difference was 59.96 mV. As shown in Figure 3a, increasing the temperature gradient between two sides of the soft TEG

https://dx.doi.org/10.1021/acsami.9b19837
ACS Appl. Mater. Interfaces 2020, 12, 17921−17928

increases the output voltage. The generated voltage can reach more than 400 mV for temperature gradients in the range of 80 °C, which was the highest temperature gradient tested. Comparing this with other previous studies on flexible TEGs, this stretchable TEG exhibits much more robust voltage output at lower and higher temperature gradients, thereby expanding the applications for this technology. Relative to a previous work, our TEG exceeds these voltage outputs significantly with values of 0.6 mV at ΔT = 10 °C (ref 13), 51.3 mV at ΔT = 19 °C (ref 15), 19 mV at ΔT = 10 °C (ref 26), 3 mV at ΔT = 20 °C (ref 27), and 8.22 mV at ΔT = 30 °C (ref 28). Moreover, the stretchable TEG presented here can be elastically strained, as described below.

In order to characterize the power generation capabilities of the LMEE TEG, the output voltage was measured across a varying external load resistor (R_{ext} = 1 to 100 Ω) for an applied temperature gradient of 60 °C (Figure 3b). In this way, the current passing through the load resistor can be calculated and used for estimating the TEG power output in the impedance matching circuit.[17,41] As shown in Figure 3b, the increase in external resistance corresponds to a sharp increase in voltage that began to level off as resistance increased well above 20 Ω. We observed that the increasing voltage soon converged with an open circuit voltage of 320 mV, that is circuits with high load resistance behave like an open circuit, as has been observed before.[42] As expected, the increase in resistance to 500 Ω corresponds to a high output voltage of 315 mV. Using these voltages and external resistances, R_{ext}, the power output is calculated as: $P = v^2/R_{ext}$. Referring to Figure 3c, the curve of this graph increases quickly and peaks at an external load of 11.5 Ω followed by a sharp drop in power as the resistance continues to increase. The TEG's maximum power for a 60 °C temperature gradient was 1.68 mW or 86.6 μW/cm^2 at the peak of 11 Ω, which corresponds to a voltage of 139 mV. Power per cm^2 of just the surface area of the semiconductors at this resistance was 0.857 mW/cm^2. The maximum power is predicted to correspond to the resistance when the internal resistance and the external load match.[15,31] This is in reasonable agreement with the experimental measurement of the internal resistance of ∼13.5 Ω at room temperature.

The internal resistance of these devices is controlled by three factors; the semiconductor resistance, the LMEE interconnect resistance, and the contact resistance between the semiconductors and interconnects. The device interconnect length was 5.48 mm with an average resistance of ∼0.12 Ω. For 101 interconnects, this gives a total value of 11.8 Ω. This average measured interconnect resistance of ∼0.12 Ω is comparable to the expected resistance value of 0.126 Ω for the same length based on the data from a previous work on LMEE electrical conductivity.[33] Likewise, ∼7 mΩ was found to be the semiconductor resistance for one semiconductor, giving ∼0.7 Ω for the 100 semiconductor array. Based on current semiconductor dimensions, the conductivity of these semiconductors is around 1.2 × 10^5 S/m. These two values for resistance along with the overall resistance for the TEG of ∼13.5 Ω give enough information to determine an expected total contact resistance of ∼1 Ω. While the resistances of commercially available TEGs are much lower, our value for device resistance is far less than or in the range with those reported in previous studies on flexible TEGs, with some research reporting resistances in the kiloOhm range.[13−17,26] The value of contact resistance is observed to be less than a tenth of the interconnect resistance. This is because of the low contact resistance between EGaIn-sputtered semiconductors and EGaIn traces, considering EGaIn is often used to mitigate contact resistances and serve as an interconnect in electronic devices.[43]

To show that these devices can remain functional under mechanical deformation, we performed tensile tests using a universal load frame (Instron 5969). Tensile tests above 50% strain along with cyclic loading tests to 30% strain were conducted. The TEGs used for the tensile measurements share the same design architecture and fabrication process described above but consisted of two rows of nine semiconductors with electrically conductive fabric connectors coming out of each end instead of the previously described 100 semiconductor units (Figure 2h). With the Instron grips in place, these slender stretchable TEGs had a gauge length of 40 mm and a width and thickness of 12.6 and 2.8 mm, respectively. Figure S1 shows one of these TEGs under stress in the universal load frame. In the first set of tests, the tensile specimens of the TEG devices were strained until electrical failure (Figure 3d). Failure occurred at strains between 50 and 70%, highlighting the stretchability of the soft TEG and its ability to support significant deformation without electrical or mechanical failure. In particular, the patterned sections of the LMEE acting as the interconnects deform with the movement of the semiconductors and maintain their connection. It should be noted that the increase of the internal resistance in these TEG devices remains below 20%, which implies a stable electrical circuit for power generation.

As shown in Figure S2, using a simplified circuit model, we predict a power loss of less than 4% for stretchable TEGs when the deviation from initial internal resistance (matched with an external resistance) remains below 35%. This level of increase or decrease of internal resistance is an equivalent to $\Delta R = \pm 5$ Ω for the fabricated TEGs with 100 semiconductors. Under the assumption of a fixed optimal load resistor, the generated power will decrease with the overall internal resistance changes because of the increase or decrease of resistance in the interconnects. The resistance change is attributed to a potential weakening/strengthening of the electrical contacts between the semiconductors and LMEE interconnects when the devices are bent, stretched, or compressed. While a variable external load resistor can address this issue by matching to the new impedance, a 30% change in internal resistance will have only modest impact on the voltage and power output. This is highly advantageous for devices that may operate under harsh conditions and under strenuous mechanical loads.

The semiconductor elements are not attributed to the increase in resistance under strain as these are rigid components. In addition, a previous work has shown that there is a minimal resistance increase under strain for LMEE traces indicting that the increase in TEG resistance under strain is not from LMEE interconnects.[34] In addition, under cyclic loading, LMEE traces have also been shown to have only a small increase in resistance.[33] This leads to the contact resistance between the traces and semiconductors as the primary source of increased resistance under strain. As shown previously for our 100-semiconductor TEGs, there exists an overall internal resistance of ∼13.5 Ω, of which ∼1 Ω is attributed to internal contact resistance. Assuming a 12% resistance increase at 50% linear strain from Figure 3d, the internal resistance will be 15.1 Ω. Considering that the increase in interconnect and semiconductor resistance is minimal, this 1.6 Ω increase in resistance is attributed to contact resistance.

https://dx.doi.org/10.1021/acsami.9b19837
ACS Appl. Mater. Interfaces 2020, 12, 17921−17928

This indicates that at a 50% strain, there is a 2.6 time increase in contact resistance. This is most likely coming from the changing morphology of the interconnects and displacement of rigid semiconductors under strain as the interconnects are thin and interfaced with semiconductors through a liquid interface. As mentioned previously, this increase in resistance at extreme strains only contributes to a 4% power loss when the deviation from the internal resistance stays below 35%.

In order to evaluate long-term performance for applications in wearable electronics, the TEG was subjected to uniaxial cyclic loading of 30% strain for 1000 cycles. A 30% strain was selected as it is the maximum typical tensile load for skin, and can be used in this case as an extreme measure for wearable applications.[23] As shown in Figure 3e, there is a slight amount of inelastic deformation with the first loading cycle, which we attribute to the Mullins effect, as has been previously shown for LMEE composites.[32] For subsequent loadings, the deformation is largely elastic, with only modest hysteresis between loading and unloading. Resistance increased as the number of cycles increased from a preloading resistance of ∼5.7 to ∼6.9 Ω (21% increase) after the 1000th 30% strain cycle (Figure 3f). Prior to loading, the stretchable TEG with only 18 semiconductors was able to generate ∼30 mV at ΔT = 75 °C. For each individual cycle, electrical resistance increased as the load increased, following the path of cyclic loading (Figure 3f). In general, the lack of permanent mechanical deformation after loading, together with the continued electrical functionality of the device under significant tensile strain, attests to LMEE's excellent applicability to soft, conformal, and stretchable thermoelectric devices.

The semiconductors in these TEGs take up 10.1% of the total area fraction. However, an increase in this area fraction, also called the fill factor, has been shown to increase the power efficiency ($W/cm^2/K^2$).[44] For commercial TEGs, a fill factor of 30% is common. Based on the current fabrication techniques, there are no barriers to increase the fill percentages of semiconductors in these TEGs to reach such an area fraction. Using the current TEG dimensions, this would require ∼300 semiconductors in a 15 by 15 grid embedded in the current sized devices. Assuming that the widths of the LMEE patterned interconnects remain the same, along with knowledge that the current parallel gap between the interconnects is ∼3.17 mm, these updated devices would have parallel interconnect gaps of 2.11 mm. This is greater than the minimum of 2 mm previously reported to avoid shorting between EGaIn traces in the LMEEs.[33] Additionally, the lengths of the interconnect traces can be shortened to keep the distance between the ends of the interconnects above 2 mm to mitigate shorting and accommodate increased semiconductors per row.

CONCLUSION

In summary, we introduce a soft and stretchable TEG that is composed of silicone rubber embedded with an array of milli-scale Bi_2Te_3 components and covered with sheets of the LMEE. The LMEE functions as both a soft and conformable heat spreader and a stretchable circuit for connecting the semiconductor components. The multifunctionality of the LMEE reduces the number of components required for electrical interconnects and addressed the poor thermal management common in flexible thermoelectric devices. Moreover, this unique fabrication process allows for a fully deformable and stretchable device that is able to operate with a limited loss of power at strains above 50% and after 1000 cycles at 30% strain. For a 60 °C temperature differential, these soft-matter TEGs generate an open circuit voltage of approximately 320 mV and a maximum power of 0.087 mW/cm^2 (1.68 mW). Even at a 10 °C temperature difference, they have an open circuit voltage of ∼60 mV. Moreover, no other soft thermoelectric devices have been tested and found to be operational without major losses of power at strain limits above 50%.

This material architecture has the ability to be expanded far beyond these initial soft TEG devices, with future opportunities to explore the integration of LMEE-based TEGs into wearable technologies. We demonstrated that the TEG devices with a LMEE thermal interface are fully conformable to be wrapped comfortably on the body and deform around the curves of the arm. To increase power, voltage, and practicality, the size of these devices can be increased and customized to various parts of the body. In the future, larger version of these devices or devices with a denser arrangement of semiconductors could be engineered into an armband-style soft TEG that could self-adhere to the skin and be used to power wearable sensors and electronic devices. This would be an opportunity to exploit the unique elasticity of these devices in order to enable on-skin energy harvesting with wearable computing systems.

EXPERIMENTAL METHODS

LMEE Fabrication. The LMEE was fabricated using a mixture of eutectic gallium indium (EGaIn; 75% gallium and 25% indium by mass) at a 50% fill ratio with a PDMS (Sylgard 184; Dow Chemicals) matrix and cured for 1 h at 100 °C.

Thermoelectric Layer. An array of doped p and n-type Bi_2Te_3 semiconductors (Wuhan Xinrong New Materials Co., Ltd.) with a purity of 99.99% were placed between the LMEE layers. The semiconductor "legs" have a dimension of 1.4 × 1.4 × 1.6 mm with a height to width aspect ratio of 1.14. To hold the legs in place and insulate between the top and bottom halves of the LMEE, the semiconductors were embedded in a PDMS center layer. For this layer, we cured Sylgard 184 with a 10:1 elastomer to curing agent ratio (by mass) in a 50 × 50 × 1.3 mm mold. The PDMS center layer was cut from the cured PDMS molds using a CO_2 laser cutter (VLS 3.50; Universal Laser Systems) and one hundred square holes for the semiconductors were cut with a dimension of 1.1 × 1.1 mm.

Voltage Output Measurements. The reported open-circuit voltage for each sample was measured as the peak voltage value obtained using an oscilloscope (Rigol DS1054Z). To ensure consistency in the measurements providing intimate contact with the hot plate and absorbing heat, a 440 g aluminum block was placed on top of the TEG.

ASSOCIATED CONTENT

Supporting Information

The Supporting Information is available free of charge at https://pubs.acs.org/doi/10.1021/acsami.9b19837.

Images of the TEG under strain in the universal load frame and the predicted power loss because of the internal resistance change in the stretched TEGs (PDF)

AUTHOR INFORMATION

Corresponding Author

Carmel Majidi − *Department of Mechanical Engineering and Department of Materials Science & Engineering, Carnegie Mellon University, Pittsburgh, Pennsylvania 15213, United States;* orcid.org/0000-0002-6469-9645; Email: cmajidi@andrew.cmu.edu

https://dx.doi.org/10.1021/acsami.9b19837
ACS Appl. Mater. Interfaces 2020, 12, 17921−17928

Authors

Mason Zadan − *Physics Department, University of Richmond, Richmond, Virginia 23173, United States*

Mohammad H. Malakooti − *Department of Mechanical Engineering, University of Washington, Seattle, Washington 98195, United States;* orcid.org/0000-0002-7187-1706

Complete contact information is available at: https://pubs.acs.org/10.1021/acsami.9b19837

Author Contributions

⊥M.Z. and M.H.M. contributed equally to this work.

Notes

The authors declare no competing financial interest.

■ ACKNOWLEDGMENTS

This material is based upon work supported by the Air Force Office of Sponsored Research under contract/grant number FA9550-18-1-0566 (Program Manager: Dr. Ken Goretta) and the National Science Foundation under contract/grant number 1635824 (Program Manager: Dr. Andrew Wells).

■ REFERENCES

(1) Suarez, F.; Nozariasbmarz, A.; Vashaee, D.; Öztürk, M. C. Designing Thermoelectric Generators for Self-Powered Wearable Electronics. *Energy Environ. Sci.* **2016**, *9*, 2099−2113.

(2) Rojas, J. P.; Singh, D.; Inayat, S. B.; Sevilla, G. A. T.; Fahad, H. M.; Hussain, M. M. Review—Micro and Nano-Engineering Enabled New Generation of Thermoelectric Generator Devices and Applications. *ECS J. Solid State Sci. Technol.* **2017**, *6*, N3036−N3044.

(3) Jung, M.; Jeon, S.; Bae, J. Scalable and Facile Synthesis of Stretchable Thermoelectric Fabric for Wearable Self-Powered Temperature Sensors. *RSC Adv.* **2018**, *8*, 39992−39999.

(4) Zhang, L.; Lin, S.; Hua, T.; Huang, B.; Liu, S.; Tao, X. Fiber-Based Thermoelectric Generators: Materials, Device Structures, Fabrication, Characterization, and Applications. *Adv. Energy Mater.* **2018**, *8*, 1700524.

(5) Schneider, F.; Fellner, T.; Wilde, J.; Wallrabe, U. Mechanical Properties of Silicones for MEMS. *J. Micromech. Microeng.* **2008**, *18*, 065008.

(6) Wei, X.; Liu, J. Power Sources and Electrical Recharging Strategies for Implantable Medical Devices. *Front. Energy Power Eng. China* **2008**, *2*, 1−13.

(7) Bahk, J.-H.; Fang, H.; Yazawa, K.; Shakouri, A. Flexible Thermoelectric Materials and Device Optimization for Wearable Energy Harvesting. *J. Mater. Chem. C* **2015**, *3*, 10362−10374.

(8) He, W.; Zhang, G.; Zhang, X.; Ji, J.; Li, G.; Zhao, X. Recent Development and Application of Thermoelectric Generator and Cooler. *Appl. Energy* **2015**, *143*, 1−25.

(9) Siddique, A. R. M.; Mahmud, S.; Heyst, B. V. A Review of the State of the Science on Wearable Thermoelectric Power Generators (TEGs) and Their Existing Challenges. *Renew. Sustain. Energy Rev.* **2017**, *73*, 730−744.

(10) Kim, S. L.; Choi, K.; Tazebay, A.; Yu, C. Flexible Power Fabrics Made of Carbon Nanotubes for Harvesting Thermoelectricity. *ACS Nano* **2014**, *8*, 2377−2386.

(11) Tomita, M.; Oba, S.; Himeda, Y.; Yamato, R.; Shima, K.; Kumada, T.; Xu, M.; Takezawa, H.; Mesaki, K.; Tsuda, K.; et al. Modeling, Simulation, Fabrication, and Characterization of a 10-MW/Cm2Class Si-Nanowire Thermoelectric Generator for IoT Applications. *IEEE Trans. Electron Devices* **2018**, *65*, 5180−5188.

(12) Gong, S.; Cheng, W. Toward Soft Skin-Like Wearable and Implantable Energy Devices. *Adv. Energy Mater.* **2017**, *7*, 1700648.

(13) Oh, J. Y.; Lee, J. H.; Han, S. W.; Chae, S. S.; Bae, E. J.; Kang, Y. H.; Choi, W. J.; Cho, S. Y.; Lee, J.-O.; Baik, H. K.; et al. Chemically Exfoliated Transition Metal Dichalcogenide Nanosheet-Based Wearable Thermoelectric Generators. *Energy Environ. Sci.* **2016**, *9*, 1696−1705.

(14) Kim, J. Y.; Oh, J. Y.; Lee, T. I. Multi-Dimensional Nanocomposites for Stretchable Thermoelectric Applications. *Appl. Phys. Lett.* **2019**, *114*, 043902.

(15) Nan, K.; Kang, S. D.; Li, K.; Yu, K. J.; Zhu, F.; Wang, J.; Dunn, A. C.; Zhou, C.; Xie, Z.; Agne, M. T.; et al. Compliant and Stretchable Thermoelectric Coils for Energy Harvesting in Miniature Flexible Devices. *Sci. Adv.* **2018**, *4*, No. eaau5849.

(16) Jo, S. E.; Kim, M. K.; Kim, M. S.; Kim, Y. J. Flexible Thermoelectric Generator for Human Body Heat Energy Harvesting. *Electron. Lett.* **2012**, *48*, 1015−1017.

(17) Hong, S.; Gu, Y.; Seo, J. K.; Wang, J.; Liu, P.; Meng, Y. S.; Xu, S.; Chen, R. Wearable Thermoelectrics for Personalized Thermoregulation. *Sci. Adv.* **2019**, *5*, No. eaaw0536.

(18) Kim, S. J.; Lee, H. E.; Choi, H.; Kim, Y.; We, J. H.; Shin, J. S.; Lee, K. J.; Cho, B. J. High-Performance Flexible Thermoelectric Power Generator Using Laser Multiscanning Lift-Off Process. *ACS Nano* **2016**, *10*, 10851−10857.

(19) Kim, C. S.; Yang, H. M.; Lee, J.; Lee, G. S.; Choi, H.; Kim, Y. J.; Lim, S. H.; Cho, S. H.; Cho, B. J. Self-Powered Wearable Electrocardiography Using a Wearable Thermoelectric Power Generator. *ACS Energy Lett.* **2018**, *3*, 501−507.

(20) Schneider, F.; Fellner, T.; Wilde, J.; Wallrabe, U. Mechanical Properties of Silicones for MEMS. *J. Micromech. Microeng.* **2008**, *18*, 065008.

(21) Dickey, M. D.; Chiechi, R. C.; Larsen, R. J.; Weiss, E. A.; Weitz, D. A.; Whitesides, G. M. Eutectic Gallium-Indium (EGaIn): A Liquid Metal Alloy for the Formation of Stable Structures in Microchannels at Room Temperature. *Adv. Funct. Mater.* **2008**, *18*, 1097−1104.

(22) Ozutemiz, K. B.; Wissman, J.; Ozdoganlar, O. B.; Majidi, C. EGaIn−Metal Interfacing for Liquid Metal Circuitry and Microelectronics Integration. *Adv. Mater. Interfaces* **2018**, *5*, 1701596.

(23) Tavakoli, M.; Malakooti, M. H.; Paisana, H.; Ohm, Y.; Green Marques, D.; Alhais Lopes, P.; Piedade, A. P.; de Almeida, A. T.; Majidi, C. EGaIn-Assisted Room-Temperature Sintering of Silver Nanoparticles for Stretchable, Inkjet-Printed, Thin-Film Electronics. *Adv. Mater.* **2018**, *30*, 1801852.

(24) Jeong, S. H.; Hjort, K.; Wu, Z. Tape Transfer Atomization Patterning of Liquid Alloys for Microfluidic Stretchable Wireless Power Transfer. *Sci. Rep.* **2015**, *5*, 8419.

(25) Dickey, M. D. Stretchable and Soft Electronics Using Liquid Metals. *Adv. Mater.* **2017**, *29*, 1606425.

(26) Chen, B.; Kruse, M.; Xu, B.; Tutika, R.; Zheng, W.; Bartlett, M. D.; Wu, Y.; Claussen, J. C. Flexible Thermoelectric Generators with Inkjet-Printed Bismuth Telluride Nanowires and Liquid Metal Contacts. *Nanoscale* **2019**, *11*, 5222−5230.

(27) Jeong, S. H.; Cruz, F. J.; Chen, S.; Gravier, L.; Liu, J.; Wu, Z.; Hjort, K.; Zhang, S.-L.; Zhang, Z.-B. Stretchable Thermoelectric Generators Metallized with Liquid Alloy. *ACS Appl. Mater. Interfaces* **2017**, *9*, 15791−15797.

(28) Suarez, F.; Parekh, D. P.; Ladd, C.; Vashaee, D.; Dickey, M. D.; Öztürk, M. C. Flexible Thermoelectric Generator Using Bulk Legs and Liquid Metal Interconnects for Wearable Electronics. *Appl. Energy* **2017**, *202*, 736−745.

(29) Sargolzaeiaval, Y.; Padmanabhan Ramesh, V.; Neumann, T. V.; Misra, V.; Vashaee, D.; Dickey, M. D.; Öztürk, M. C. Flexible Thermoelectric Generators for Body Heat Harvesting—Enhanced Device Performance Using High Thermal Conductivity Elastomer Encapsulation on Liquid Metal Interconnects. *Appl. Energy* **2020**, *262*, 114370.

(30) Kazem, N.; Hellebrekers, T.; Majidi, C. Soft Multifunctional Composites and Emulsions with Liquid Metals. *Adv. Mater.* **2017**, *29*, 1605985.

(31) Malakooti, M. H.; Kazem, N.; Yan, J.; Pan, C.; Markvicka, E. J.; Matyjaszewski, K.; Majidi, C. Liquid Metal Supercooling for Low-Temperature Thermoelectric Wearables. *Adv. Funct. Mater.* **2019**, *29*, 1906098.

(32) Bartlett, M. D.; Kazem, N.; Powell-Palm, M. J.; Huang, X.; Sun, W.; Malen, J. A.; Majidi, C. High Thermal Conductivity in Soft Elastomers with Elongated Liquid Metal Inclusions. *Proc. Natl. Acad. Sci. U.S.A.* **2017**, *114*, 2143−2148.
(33) Markvicka, E. J.; Bartlett, M. D.; Huang, X.; Majidi, C. An Autonomously Electrically Self-Healing Liquid Metal−Elastomer Composite for Robust Soft-Matter Robotics and Electronics. *Nat. Mater.* **2018**, *17*, 618−624.
(34) Fassler, A.; Majidi, C. Liquid-Phase Metal Inclusions for a Conductive Polymer Composite. *Adv. Mater.* **2015**, *27*, 1928−1932.
(35) Champier, D. Thermoelectric Generators: A Review of Applications. *Energy Convers. Manage.* **2017**, *140*, 167−181.
(36) Goldsmid, H. Bismuth Telluride and Its Alloys as Materials for Thermoelectric Generation. *Materials* **2014**, *7*, 2577−2592.
(37) Chen, Y.; Hou, X.; Ma, C.; Dou, Y.; Wu, W. Review of Development Status of Bi2Te3-Based Semiconductor Thermoelectric Power Generation https://www.hindawi.com/journals/amse/2018/1210562/abs/ (accessed Dec 30, 2019).
(38) Hu, L.-P.; Zhu, T.-J.; Wang, Y.-G.; Xie, H.-H.; Xu, Z.-J.; Zhao, X.-B. Shifting up the Optimum Figure of Merit of p -Type Bismuth Telluride-Based Thermoelectric Materials for Power Generation by Suppressing Intrinsic Conduction. *NPG Asia Mater.* **2014**, *6*, No. e88.
(39) Tan, S. H.; Nguyen, N.-T.; Chua, Y. C.; Kang, T. G. Oxygen Plasma Treatment for Reducing Hydrophobicity of a Sealed Polydimethylsiloxane Microchannel. *Biomicrofluidics* **2010**, *4*, 032204.
(40) Zhou, J.; Khodakov, D. A.; Ellis, A. V.; Voelcker, N. H. Surface Modification for PDMS-Based Microfluidic Devices. *Electrophoresis* **2012**, *33*, 89−104.
(41) Malakooti, M. H.; Patterson, B. A.; Hwang, H.-S.; Sodano, H. A. ZnO Nanowire Interfaces for High Strength Multifunctional Composites with Embedded Energy Harvesting. *Energy Environ. Sci.* **2016**, *9*, 634−643.
(42) Malakooti, M. H.; Zhou, Z.; Sodano, H. A. Enhanced Energy Harvesting through Nanowire Based Functionally Graded Interfaces. *Nano Energy* **2018**, *52*, 171−182.
(43) Harada, S.; Arie, T.; Akita, S.; Takei, K. Highly Stable Liquid−Solid Metal Contact Toward Multilayered Detachable Flexible Devices. *Adv. Electron. Mater.* **2015**, *1*, 1500080.
(44) Condos, A. P.; Zimaras, L.; Marlow, J.; Kurniawan, M. Optimisation of Wearable Thermoelectric Generators. *PAM Rev. Energy Sci. Technol.* **2019**, *6*, 2−15.

https://dx.doi.org/10.1021/acsami.9b19837
ACS Appl. Mater. Interfaces 2020, 12, 17921−17928